Indirect Toll-like receptor 5-mediated activation of conventional dendritic cells promotes the mucosal adjuvant activity of flagellin in the respiratory tract

Delphine Fougeron, Laurye van Maele, Pascal Songhet, Delphine Cayet, David Hot, Nico van Rooijen, Hans-Joachim Mollenkopf, Wolf-Dietrich Hardt, Arndt G. Benecke, Jean-Claude Sirard

Indirect Toll-like Receptor 5-mediated activation of conventional dendritic cells promotes the mucosal adjuvant activity of flagellin in the respiratory tract[1]

Delphine Fougeron[*,†,‡,§], Laurye Van Maele[*,†,‡,§], Pascal Songhet[¶], Delphine Cayet[*,†,‡,§], David Hot[*,†,‡,§], Nico Van Rooijen[‖], Hans-Joachim Mollenkopf[#], Wolf-Dietrich Hardt[¶], Arndt G. Benecke[**], and Jean-Claude Sirard[*,†,‡,§,††]

[1]DF, LVM, JT, DC and JCS were funded by INSERM, Institut Pasteur de Lille, Région Nord Pas de Calais (Ph.D. fellowship), Université de Lille, the European Community (STREP "SavinMucoPath" INCO-CT-2006-032296 and "FLAGMARK" TRANSVAC grant agreement n°228403), and Inserm Transfert. AGB was funded by the Agence Nationale pour la Recherche (Physio2007 n°013-01) and the Genopole Evry.

[*]Institut Pasteur de Lille, Centre d'Infection et d'Immunité de Lille, F-59000 Lille, France; [†]Institut National de la Santé et de la Recherche Médicale, U1019, F-59000 Lille, France; [‡]Centre National de la Recherche Scientifique, UMR 8204, F-59000 Lille, France; [§]Université de Lille, F-59000 Lille, France; [¶]Institute of Microbiology, Eidgenössische Technische Hochschule Zürich, CH-8093 Zürich, Switzerland; [‖]Department of Molecular Cell Biology, VU Medical Center, Amsterdam, The Netherlands; [#]Max Planck Institute for Infection Biology, Berlin, Germany; [**]Institut des Hautes Études Scientifiques and Centre National de la Recherche Scientifique, F-91440 Bures-sur-Yvette, France;

[††]Correspondence: Jean-Claude Sirard, e-mail: jean-claude.sirard@inserm.fr

Running title: Nasal flagellin activates lung conventional dendritic cells

Wordcount: 3000

Abstract

The toll-like receptor 5 agonist (TLR5) flagellin is an effective adjuvant for vaccination. Recently, we demonstrated that the adaptive responses stimulated by intranasal administration of flagellin and antigen were linked to TLR5 signaling in the lung epithelium. The present study sought to identify the antigen presenting cells involved in this adjuvant activity. We first found that the lung dendritic cells captured antigen very efficiently in a process independent of TLR5. However, TLR5-mediated signaling specifically enhanced the maturation of lung dendritic cells. Afterward, the number of antigen-bound and activated conventional dendritic cells (both $CD11b^+$ and $CD103^+$) increased in the mediastinal lymph nodes in contrast to monocyte-derived dendritic cells. These data suggested that flagellin-activated lung conventional dendritic cells migrate to the draining lymph nodes. The lymph node dendritic cells, in particular $CD11b^+$ cells, were essential for induction of CD4 T-cell response. Lastly, neutrophils and monocytes were recruited into the lungs by flagellin administration but did not contribute to the adjuvant actvity. The functional activation of conventional dendritic cells was independent of direct TLR5 signaling, thereby supporting the contribution of maturation signals produced by flagellin-stimulated airway epithelium. In conclusion, our results demonstrated that indirect TLR5-dependent stimulation of airway conventional dendritic cells is essential to flagellin's mucosal adjuvant activity.

Wordcount: 205

Introduction

Many pathogens of public health concern colonize the respiratory tract in general and the lung mucosa in particular. Mucosal vaccines induce a local adaptive immune response (i.e. secretory antibodies and mucosal T cells) and constitute a unique means of preventing these infections [1]. The few commercially available mucosal vaccines contain live attenuated pathogens and are effective. However, so far mucosal adjuvant candidates to be formulated with subunit vaccines have not demonstrated sufficient levels of potency and safety.

Most vaccines are delivered systemically and use systemic adjuvants. In recent years, it appears that these adjuvants mimic activation of immunity by live microorganisms and thereby enhance appropriate memory responses to infections [2, 3]. A common feature is the transient induction of an innate pro-inflammatory response [2, 4-7]. Thus, adjuvants like MF59 and alum trigger the infiltration of polymorphonuclear neutrophils (PMNs) and antigen-presenting cells (APCs, i.e. inflammatory monocytes and/or dendritic cells (DCs)) at the injection site [5, 8-11]. They specifically induce the functional maturation of APCs, thereby promoting functions related to antigen presentation.

Dendritic cells (DCs) are the most professional APCs that drive adjuvant activity [12]. In non-lymphoid tissues (such as lung) and at steady state, conventional DCs (cDCs) that originate from a pre-DC precursor serve as sentinels [13]. cDCs are characterized by the expression of CD11c, MHCII, CD24 and ZBTB46 and one can distinguish in the lungs between $CD11b^+$ and $CD103^+$ cDCs [13, 14]. When activated by systemic adjuvants, tissue DCs migrate to draining lymph nodes and give rise to migratory DCs that trigger adaptive immunity [15-18]. The $CD11b^+$ cDCs are mainly associated with the trigger of Th2 responses, whereas $CD103^+$ cDCs rather promote Th1/Th17 responses and cross-presentation [17, 19-21]. Upon vaccination or infection, inflammatory monocytes that have entered tissues via CCR2 can also differentiate into DCs [10-12, 22]. These monocyte-derived DCs (moDCs) express not only CD11c and MHCII but also CD11b and the monocyte/macrophage marker CD64. However they lack CD24 [17, 23]. Depending on the adjuvant or the inflammatory injury, moDCs elicit or reactivate CD4 and CD8 T cell responses [8, 11, 24]. To develop safe and potent mucosal

77 vaccines, it is thus necessary to determine their impact on cDCs and moDCs recruitment and
78 activation.

79 Toll-like receptors (TLRs) are essential for the activation of adaptive immunity by DCs and
80 TLR agonists represent therefore potent adjuvant candidates for future vaccines. Flagellins are
81 detected by TLR5, which in turn drives adjuvant activity via systemic and mucosal immunization
82 routes [25]. When delivered by systemic route, flagellin directly stimulates the maturation of spleen
83 DCs and thus activates T and B cell responses [26-28]. When flagellin is administered by the
84 intranasal (i.n.) route, radioresistant cells of the lung epithelium expressing TLR5 control the innate
85 immune responses [29, 30]. Recently, the antibody and CD4 T cell responses stimulated i.n. by
86 flagellin as a mucosal adjuvant were linked to TLR5 signaling in the lung epithelium [30, 31]. Hence,
87 this study aims at characterizing the APCs involved in flagellin's mucosal activity.
88

Materials and methods

Mice and reagents. Animals were maintained in a specific pathogen-free facility (#A59-350009, Institut Pasteur de Lille) and all experiments complied with national regulations and ethical guidelines. Six to 10-weeks-old mice (C57BL/6, C3H/HeN, *Tlr5*$^{-/-}$, *Cd11c-DTR*, CD45.1, OT-II on the C57BL/6 background) were obtained from Janvier, Charles River or bred in house. To generate bone marrow (BM) chimeric mice, wild type C57BL/6 (WT) or *Tlr5*$^{-/-}$ mice were lethally irradiated (11 Gray) and intravenously (i.v.) injected with 3-5 x10^6 BM cells. After 12-14 weeks, the reconstitution was assessed by flow cytometry using CD45.1 and CD45.2 markers. Flagellin (FliC) from *Salmonella enterica* Serovar Typhimurium, as well as "flagellin$_{TLR5mut}$" (signaling motif [QRVRELAV] changed in the non signaling motif [DTVKVKAT]) were prepared as described [32]. Endograde ovalbumin (OVA) was purchased from Hyglos, AlexaFluor® 647 ovalbumin (OVA-AF647) from Molecular Probes and Hen Egg Lysosyme (HEL) from Appligene. All proteins were free of or depleted of endotoxin activity using Triton X-114 and/or Detoxi-Gel Affinity Columns (Pierce).

Immunization and sampling. Mice were anesthetized by intraperitoneal (i.p.) injection of ketamine-xylazine and immunized i.n. with 30µL of PBS containing OVA (10µg), OVA-AF647 (30µg) or HEL (800µg) ± flagellin (1µg). Mice were euthanized by i.p. injection of sodium pentobarbital and perfused lungs, MdLNs, cervical lymph nodes (CLN), spleen, or blood were collected. Intravenous injection of CD45-PE-Cy7 antibody was performed 5min prior to sampling to specifically label vasculature-associated or marginated cells [33]. To deplete DC, *Cd11c-DTR* → WT mice were i.p. injected with 600ng and 200ng diphtheria toxin (DTX) 48h and 24h respectively before i.n. immunization as described [34].

Flow cytometry. Cells were isolated from tissues by digestion with collagenase IA (1mg/mL, Sigma) and DNAse I (40µg/ml, Sigma) for 30 min at 37°C. The lung hematopoietic cells were recovered after centrifugation on Percoll 20%. After incubation with anti-CD16/CD32 Fc block (2.4G2), cells were stained with specific antibodies: CD45 (30F11), CD3ε (145-2C11), CD19 (1D3), CD4 (RM4-5), Vα2-

TCR (B20.1), CD11c (N418), CD24 (M1/69), CD64 (X54-5/7.1), MHCII (M5/114.5.2) specific for I-A^b/I-E^b/I-A^k, CD103 (2E7), CD11b (M1/70), Ly6C (AL21), Ly6G (1A8), CCR2 (475301), CD86 (GL-1), CD80 (16-10A1) (Becton Dickinson, BioLegend and eBioscience). C4H3-biotinylated antibody was used to detect HEL_{46-61} peptide loaded on I-A^k [26, 35]. Intracellular staining of IL-12 p40 (C15.6) was performed using cells incubated for 3h at 37°C with brefeldin A (1µg/mL, Sigma-Aldrich) and fixation/permeabilization kit from eBioscience. Data were collected on a BD LSR Fortessa and analyzed with BD FACSDiva or FlowJo. Cells were sorted on a BD FACSAria.

Adoptive transfer of CD4 T cells. CD4 lymphocytes were isolated from lymphoid organs of OT-II mice by negative selection (CD4 isolation kit, Miltenyi Biotec). Cells were stained with 5µM of carboxyfluorescein diacetate succinimidyl ester (CFSE) or 10µM of CellTrace™ Violet (CTV) (Invitrogen) and 5×10^6 cells were injected intravenously into animals. One day later, mice were immunized i.n. with PBS or OVA (20µg) ± flagellin. Tissues were sampled at day 5 for analysis of fluorescence dilution in T cells.

Antigen presentation assays. C57BL/6 mice were immunized i.n. with flagellin and OVA (47.5µg), MdLNs were sampled 18h later, and APCs were FACS sorted. APCs were cultured in round bottom 96 wells plate with 3-5×10^5 CTV-stained OT-II cells at a ratio of 1:10. At day 5, cell proliferation was assessed by flow cytometry. The cytokines IL-13 and IFN-γ were detected in supernatants using ELISA kits (eBioscience).

Statistical analysis. Results are expressed as mean ± SEM. Mann-Whitney test was used to assess statistically significant between groups.

Results

Flagellin promotes the recruitment of conventional dendritic cells into lung draining lymph nodes

To dissect flagellin's mode of action as an i.n. adjuvant, we investigated the early dynamic of lung DCs including cDCs and moDCs, as well as monocytes and PMNs (**Fig.1**). As previously described [29, 36, 37], our experiments revealed a recruitment of PMNs ($Ly6C^{+}Ly6G^{+}$) as early as 3h post-instillation that peaked at 6h (**Fig.1B**). Monocytes ($Ly6G^{neg}Ly6C^{+}$) were recruited by flagellin treatment in similar kinetics. These cells were also found to express CCR2 and CX3CR1, features of inflammatory monocytes (**data not shown**). In contrast, we observed a consistent but not significant decrease in the numbers of lung $CD11b^{+}$ or $CD103^{+}$ DCs at 6h (**Fig.1B**). Analysis of lung $CD11b^{+}$ DC revealed that cDC ($CD24^{+}$) and moDC ($CD64^{+}$) were similarly altered by flagellin immunization. Interestingly, the increase of lung monocyte counts was not associated with similar changes in moDCs, suggesting that monocytes did not give rise to moDC.

The MdLNs that drain the lung are known to be a major site for the induction of T cell-mediated immunity following flagellin administration [30, 31]. Relative to the lungs, significant changes in the MdLN counts of $CD11b^{+}$ and $CD103^{+}$ DCs were observed after i.n. administration of flagellin or flagellin plus antigen, relative to controls (**Fig.1C-D**). The changes in DC numbers were observed after 18h treatment (but not after 6h) and rapidly returned to baseline. We further established that the increase of MdLN $CD11b^{+}$ DCs was due to cDCs but not moDCs, given their expression of CD24 and the lack of CD64 expression (**Fig.1E**). Importantly, DC recruitment was not detected in the CLNs draining the nasal cavity (**Fig.1F**). In summary, intranasal administration of flagellin triggers an early recruitment of PMN and monocytes into the lung and an increase of cDC numbers in MdLNs.

Antigen-bound dendritic cells predominates in the airways and draining lymph nodes

In order to track the cells that had captured the antigen, fluorescent ovalbumin (OVA-AF647) was administered intranasally (**Fig.2**). As early as 3h post-immunization, lung cells were associated with the fluorescent antigen (**data not shown**). Six hours post-administration of OVA-AF647, we found that 50% of $CD11b^{+}$ DCs, 70% of $CD103^{+}$ DCs, 20% of PMNs and 10% of monocytes were

bound to antigen (**Fig.2A**). Remarkably, the same proportion of antigen-bound cells was found 6h after administration of flagellin plus OVA-AF647. However, the number of monocytes and PMNs bound to OVA increased >3-fold and >20-fold, respectively, thereby correlating with the magnitude of these cells' infiltration (**Fig.2B**). In contrast, the $CD11b^+$ and $CD103^+$ DC counts bound to OVA did not change significantly after flagellin treatment. We also investigated the localization of OVA-bound lung cells by injecting an intravenous pulse of CD45-specific antibody (**Fig.2C-D**). Interestingly, antigen-bearing monocytes were mostly marginated (i.e. in the vasculature) whereas DCs were mostly interstitial. In contrast, PMNs shifted from marginated to interstitial position after flagellin stimulation, revealing the translocation of PMN into the bronchoalveolar compartment. Taken as a whole, these data suggest that lung DCs have a key role in antigen capture following intranasal vaccination.

We next investigated whether cells that had captured fluorescent OVA can be found in the MdLNs. In contrast to lungs, we did not detect any significant changes of DC harboring antigen in the MdLN 6h post-administration of flagellin (**data not shown**). However, the number of OVA-bound $CD11b^+$ and $CD103^+$ MdLN DCs was significantly enhanced at 18h (**Fig.3A**). We did not detect any antigen-bound PMN or monocytes in MdLN. Moreover, there was not any flagellin-dependent increase of antigen-bound cells in the CLNs draining the nasal cavity. These observations suggest that antigen capture by lung DC is followed by migration of cDC into MdLN.

Finally, we assessed the potential contribution of infiltrating monocytes or PMNs to flagellin's adjuvant activity by performing experiments with clodronate liposomes, *Ccr2*$^{-/-}$ mice and Ly6G-specific depleting antibodies (**Supplementary Fig.1**). Animals depleted or deficient in PMNs or monocytes responded in much the same way as control animals did to i.n. immunization - suggesting that monocytes and PMNs do not modulate the adjuvant activity.

Dendritic cells are functionally activated by flagellin

Since lung DCs from control and flagellin-immunized animals captured similarly antigen, we next assessed whether flagellin impact on DC activation Microarray analysis of transcriptional changes over time in lung highlighted that the DC maturation pathway and the functions related to antigen presentation were upregulated (**Supplementary Fig.2**). In contrast, these patterns were not

observed in the blood. We next observed that both $CD11b^+$ and $CD103^+$ lung cDCs upregulated the expression of MHCII and the co-stimulatory molecules CD80 and CD86 as soon as 6h post-immunization (**Supplementary Fig.3A-C**). In addition, the lung cDCs upregulated functions of processing and presentation of antigen since immunization with hen egg lysozyme (HEL) and flagellin significantly increased staining with the C4H3 antibody that recognizes the MHCII-loaded HEL_{46-61} (**Supplementary Fig.3D**).

The flagellin administration was also associated with functionally activated cDCs in MdLNs 18h post-immunization as evaluated by the upregulation of CD80, CD86 as well as C4H3 staining (**Fig.3B-D**). Lastly, MdLN $CD11b^+$ but not $CD103^+$ cDCs were shown to produce the T-cell activating cytokine IL-12 p40 (**Fig.3E-F**). Altogether, these results suggest that flagellin signaling enhances the functional activation of lung cDCs and their migration to the MdLNs.

$CD11b^+$ cDCs are crucial for the flagellin-mediated $CD4^+$ T cell activation

To ascertain the role of cDCs, we performed experiments with chimera mice harboring *Cd11c-DTR* bone marrow that can be injected with DTX to eliminate lung DCs (**Fig.4A**). Passively transferred, OVA-specific $CD4^+$ OT-II cells were monitored as a guide to adjuvant activity. Flagellin and OVA strongly stimulated the proliferation of OT-II cells both in MdLNs from control wild type animals and control *Cd11c-DTR* chimera animals (**Fig.4B-C**). DTX treatment of *Cd11c-DTR* mice prior to immunization abrogated the proliferation of the OT-II cells. Interestingly, DC depletion did not impact on the flagellin-mediated lung innate response, as assessed by production of the chemokine CCL20 (**Fig.4D**). Therefore, these data strongly suggest that mucosal cDCs are essential for the adjuvant activity of i.n. flagellin.

The cDCs' ability to present antigen was further analyzed *in vitro*. OT-II lymphocytes were cultured with total DCs, $CD11b^+$ or $CD103^+$ DCs that were sorted from the MdLNs of animals immunized i.n. with flagellin and OVA. We found that $CD11b^+$ DCs efficiently activated OT-II cells and thus prompted them to proliferate and secrete the T cell-specific cytokines IFNγ and IL-13. In these conditions, $CD103^+$ DCs hardly stimulated proliferation or cytokine production (**Fig.4E-G**). Similar results were obtained by injecting sorted MdLN DCs into mice adoptively transferred with

OT-II cells (**Supplementary Fig.4**). These data demonstrated that $CD11b^+$ MdLN cDCs are essential components in the flagellin's adjuvant activity by stimulating $CD4^+$ T cell responses.

Direct TLR5 signaling in DCs is not required for the cells' functional activation

Intranasal adjuvant activity of flagellin depends on TLR5 and is abrogated in *Tlr5*$^{-/-}$ mice or mice immunized with flagellin mutated within the TLR5 motif, i.e. flagellin$_{TLR5mut}$ [30, 32]. We therefore studied whether flagellin-mediated MdLN DC activation depends on TLR5 signaling. Notably, we did not detect any activation of MdLN cDCs in *Tlr5*$^{-/-}$ mice in contrast to the situation in WT animals (**Fig.5A-B**). Similarly, intranasal immunization of WT animals with flagellin$_{TLR5mut}$, did not induce any activation of MdLN DCs in contrast to native flagellin (**Fig.5C**).

To determine whether nasal administration of flagellin directly activate airway DCs, we generated chimeric mice by transferring a combination of *Tlr5*$^{-/-}$ and WT bone marrow (**Fig.5D**). Activation was measured by the expression of co-stimulatory molecules in CD45.1-expressing DC (i.e. WT) and CD45.2-expressing DC (i.e. *Tlr5*$^{-/-}$). As previously reported, intraperitoneal administration of flagellin only induced activation of WT spleen DC but not *Tlr5*$^{-/-}$ DC (**Fig.5E**). This systemic DC activation was therefore a process dependent on direct TLR5 signaling. In contrast, after intranasal flagellin administration, MdLN DC activation occurred independently of TLR5 expression on DCs (**Fig.5F-G**), indicating that *Tlr5*$^{-/-}$ MdLN DC are transactivated by WT cells. Using chimera where *Tlr5*$^{-/-}$ animals were transferred with WT cells and the opposite condition, we found that MdLN DC activation required *Tlr5* expression in the radioresistant cell compartment (**Supplementary Fig.5**). Interestingly, *Tlr5* mRNA levels were respectively 8-fold lower in lung DC compared to airway epithelial cells (**Supplementary Fig.5**). In summary, these data suggest that flagellin's effect on cDC activation was independent of direct TLR5 signaling in DCs but requires instruction by TLR5-dependent mechanisms in epithelial cells.

Discussion

The development of novel prophylactic strategies requires knowledge of the APCs involved in vaccine efficacy. Our present results demonstrate that the intranasal adjuvant activity of flagellin is linked to the functional activation of lung DCs and MdLN cDCs. Our data suggest that flagellin enhances the ability of lung cDC to present antigen and to migrate to draining lymph nodes for $CD4^+$ lymphocyte stimulation. Furthermore, cDC activation does not involve direct TLR5 signaling but is likely dependent on transactivation signals originating from TLR5-expressing airway epithelial cells. Finally, we provided strong evidence that transactivation does not rely on the expression of IL-25, TSLP, IL-33, IL-1α, IL-1β, or IL-36γ.

How DCs are activated is an important parameter in the development of adjuvants. A prominent concept is the direct activation of DCs by adjuvants [38]. The mucosal activity of flagellin requires epithelial TLR5 signaling in airways [29, 30]. The present data indicate that DCs are not the target cells of flagellin since they are activated by indirect TLR5 rather than direct TLR5 signaling, reinforcing the contribution of airway epithelium as flagellin target. This contrasts with the systemic route of flagellin immunization that directly stimulate TLR5 signaling in DCs (**Fig.5 and Supplementary Fig.5**) [27, 39]. Airway epithelial cells were also found essential to induce the DC activation in response to respiratory delivery of TLR4-dependent allergen that leads to asthma [40]. Epithelial cytokines that activate lung DCs in response to mucosal challenge have been identified [41-44]. Defining the epithelial factors involved in the adjuvant effect of flagellin will open up unprecedented avenues in the vaccine field.

Our results demonstrated that lung DCs are activated and that MdLN cDCs, particularly $CD11b^+$ cDCs present antigen to $CD4^+$ T cells. The counts of MdLN cDCs rose during immunization and thus supported the migration of lung cDCs to lymph nodes. Lung cDCs efficiently capture antigen in absence of any stimulation since they are ideally positioned for antigen sampling [45]. Our data demonstrate that the main activity of flagellin as an adjuvant is to functionally activate DCs. Consistently, $CD11b^+$ DC have a key role in the mucosal adjuvant activity of cholera toxin [46].

The lung transcriptional signature induced by intranasal administration of flagellin shares features of various adjuvants [5-7, 21]. Adjuvants generally upregulate the pathways of acute phase

response and chemokine signaling, highlighting the recruitment of inflammatory cells. PMNs are mobilized in response to flagellin and the process is linked to the production of chemokines by the epithelial TLR5 signaling pathway [29, 36]. Our data suggest that PMNs do not regulate the flagellin's adjuvant activity (as for the adjuvant MF59 [47]). Flagellin administration also promoted the recruitment of monocytes into lung but monocytes and moDCs are not required for flagellin-mediated activity. It is noteworthy that in asthma, high doses of allergen stimulates lung moDC migration to the lymph nodes [20]. In our setting, the low antigen doses and the transient innate response stimulated by flagellin may impair differentiation into moDCs. The observation that flagellin's adjuvant activity is dissociated from inflammatory cell recruitment is a fascinating perspective for vaccine improvement.

The development of mucosal adjuvants requires a detailed understanding of the transactivating factors and the signals that bypass the tolerogenic imprinting of the mucosa on DCs. In conclusion, this study opens up new avenues for designing safer adjuvants with a less intense pro-inflammatory response and fewer side effects.

Acknowledgements

We thank Dr. C. Faveeuw for critical reading of the manuscript, Dr. F. Trottein for *Cd11c-DTR* mice, Dr. R. Steinman for C4H3-specific antibodies, Dr. David Hot for technical assistance in IPA analysis, Julien Tabareau for flagellin production, and Emeric Deruy and Bioimaging Center Lille-Nord de France for flow cytometry and cell sorting, respectively.

Authorship

Contribution: D.F. planned studies, performed experiments, analyzed data, and wrote the manuscript; L.V.M. performed experiments and analyzed data. D.C. and P.S. performed experiments. N.V.R., and W.D.H. contributed vital reagents. DH, H.J.M. and A.G.B. performed experiments and analyzed microarray data. J.C.S. supervised the project and wrote the manuscript.

Conflict-of-interest disclosure: The authors declare no competing financial interests.

Correspondence: Jean-Claude Sirard, Institut Pasteur de Lille, Centre d'Infection et d'Immunité de Lille, Equipe Infection Pulmonaire et Immunité Innée, 1 rue du Professeur Calmette, 59019 Lille Cedex, France; e-mail: jean-claude.sirard@inserm.fr

Figure legends

Figure 1: Analysis of recruitment of neutrophils, monocytes and dendritic cells into the lungs and draining lymph nodes following flagellin immunization. C57BL/6 mice (n=4) were treated i.n. with either flagellin, ovalbumin (OVA), or flagellin plus OVA. Lung, mediastinal (MdLN) or cervical (CLN) lymph nodes samples were collected at the indicated time points for flow cytometry analysis. (A) Gating strategy for the identification of lung cells. After gating on $CD45^+$, lung cells were identified as follows: cDCs ($lin^{neg}CD11c^+MHCII^+CD24^+CD11b^{+/neg}CD103^{+/neg}$), moDCs ($lin^{neg}CD11c^+MHCII^+CD64^+CD11b^+$), monocytes ($CD11b^{high}Ly6C^{high}Ly6G^{neg}$) and PMNs ($CD11b^{high}Ly6C^+Ly6G^+$). The same strategy was used for MdLN and CLN cells. (B,C) Absolute counts of lung total PMNs, monocytes, $CD11b^+$ cDCs, moDCs, and $CD103^+$ cDCs over time in lungs (B) and MdLNs following flagellin immunization (C). (D) Numbers of $CD11b^+$ and $CD103^+$ DC in MdLNs 18h post-immunization with OVA or flagellin plus OVA. (E) Analysis of composition of $CD11b^+$ DC in MdLNs. (F) Numbers of $CD11b^+$ and $CD103^+$ DC in CLNs 18h post-immunization with OVA or flagellin plus OVA. Results are expressed as the mean ± SEM and are representative of 2-5 experiments (* p <0.05).

Figure 2: Analysis of antigen uptake by lung neutrophils, monocytes and dendritic cells. C57BL/6 mice (n=4) were treated i.n. with fluorescent ovalbumin (OVA-AF647) in the presence or absence of flagellin. Lung samples were collected at 6h for flow cytometry analysis. (A) Absolute counts of OVA-positive PMNs ($CD45^+CD11b^{high}Ly6C^+Ly6G^+$), monocytes ($CD45^+CD11b^{high}Ly6C^{high}Ly6G^{neg}$), $CD11b^+$ and $CD103^+$ DCs ($lin^{neg}CD45^+CD11c^+MHCII^+CD11b^{+/neg}CD103^{+/neg}$). (B) Representative histograms of antigen uptake by cell type. For each cell type, the number indicates the percentage of OVA-positive cells among the total population considered. (C-D) Six hours post-immunization, mice were injected i.v. with anti-CD45-PeCy7 (1µg) and lung tissues were sampled 5 minutes later. Cells stained by anti-CD45-PeCy7 are defined as marginated cells. (C) Percentage of margination was determined for monocytes, DC, and PMN. (D) Representative plots showing the correlation between antigen uptake and cell

localization. Results are expressed as the mean ± SEM, and are representative of 2-4 experiments (* p <0.05).

Figure 3: Draining lymph nodes CD11b$^+$ cDC process antigens and exhibit functional maturation after flagellin intranasal administration. Mice (n=3-4) were immunized i.n. and mediastinal lymph nodes (MdLN) were sampled at 18h for flow cytometry analysis. Dendritic cells were defined as lin^{neg}CD45$^+$CD11c$^+$MHCII$^+$CD11b$^{+/-}$CD103$^{+/-}$. (A-C) C57BL/6 animals were immunized i.n. with fluorescent ovalbumin (OVA-AF647) or flagellin and OVA-AF647. (A) Absolute numbers of antigen-positive MdLN DCs. (B) Representative histograms of CD80 and CD86 expression by MdLN DCs. (C) Quantitative analysis of CD86 expression in DCs. (D) C3H/HeN animals were immunized i.n. with either hen egg lysozyme (HEL), flagellin, or flagellin and HEL. Antigen presentation by DCs was assessed with C4H3 antibody that detects HEL peptide loaded on I-A^k. Fluorescence of the C4H3 antibody was normalized against the I-A^k fluorescence. (E-F) C57BL/6 were immunized i.n. with PBS or flagellin. (E) Representative histograms of IL-12 p40-producing DCs. (F) Percentage of IL-12 p40-producing CD11b$^+$ and CD103$^+$ DC among the total population of DC. Results are expressed as the mean ± SEM and are representative of 2-4 experiments (* p <0.05).

Figure 4: CD11b$^+$ dendritic cells are essential for flagellin's mucosal adjuvant activity.
(A-D) C57BL/6 (WT) and *Cd11c*-DTR → WT chimera mice (n=3-4) were treated twice i.p. with PBS or diphtheria toxin (DTX) (200 ng 24h before immunization and 600 ng at immunization). (A) Representative plots of DC depletion in the spleen and lung. Using flow cytometry, dendritic cells were defined as lin^{neg}CD45$^+$CD11c$^+$MHCII$^+$CD11b$^{+/-}$CD103$^{+/-}$. Numbers indicate the DC as percentage of CD45$^+$ cells 24h after DTX injection. (B-C) WT and *Cd11c*-DTR → WT mice were adoptively transferred with CFSE-labeled OT-II CD4$^+$ T cells that are specific for ovalbumin (OVA) and treated i.p. with DTX or PBS. After 24h, Animals were immunized i.n. with PBS or flagellin and OVA and treated i.p. with DTX or PBS. The proliferation of OT-II cell was analyzed 5 days after immunization in the spleen and the mediastinal lymph nodes (MdLN). Abrogation of T cell response by DC depletion is shown as representative plots (B) and quantification of division (C). Plots show the CFSE fluorescence of CD4$^+$Vα2$^+$ OT-II cells and are representative of two experiments. (D) Lung

innate response to flagellin after DC depletion. WT and *Cd11c*-DTR → WT mice were DTX-treated and immunized i.n. with PBS or flagellin and OVA. CCL20 production was measured in the serum 6h after the i.n. administration as a marker of lung activation. (E-G) C57BL/6 mice (n=16) were immunized i.n. with flagellin and OVA and the MdLN were sampled 18h later. DCs were sorted as the total DC population ($lin^{neg}CD45^{+}CD11c^{+}MHCII^{+}$), $CD11b^{+}$ and $CD103^{+}$ DC subsets. DCs (5×10^{4}) were cultured with CTV-labeled OT-II cells (5×10^{5}) for 5 days. (E-F) T cell proliferation induced by DCs is shown as representative histograms of CTV dilution (E) and quantification of division as a percentage of total OT-II cells (F). (G) Analysis of cytokine production in the DC-OT-II co-culture supernatants. The results are representative of three experiments (* $p < 0.05$).

Figure 5: Dendritic cell maturation following intranasal administration of flagellin does not require direct activation through TLR5 signaling.

(A-B) *Tlr5*$^{-/-}$ or C57BL/6 (WT) mice (n=3-4) were immunized i.n. with PBS or flagellin. (C) C57BL/6 mice (n=3-4) were immunized i.n. with PBS, flagellin or flagellin mutated for the TLR5 signaling motif ($flagellin_{TLR5mut}$). Cells isolated 18h after immunization from mediastinal lymph nodes (MdLN) were analyzed by flow cytometry. Dendritic cells (DC) were defined as $lin^{neg}CD45^{+}CD11c^{+}MHCII^{+}CD11b^{+/-}CD103^{+/-}$. (A-C) Quantitative analysis of CD80 and CD86 expression. (D) Experimental strategy of mixed bone marrow chimera. Bone-marrow from *Tlr5*$^{-/-}$ [CD45.2] and WT [CD45.1] (1:1 ratio) animals were injected into lethally irradiated WT [CD45.2] mice. Three months after engraftment (>95% reconstitution of DC compartment), chimera mice (n=3-5) were immunized with flagellin by intravenous (E) or intranasal route (F-G). The functional maturation of spleen DC (E) or MdLN DC (F-G) was assessed 18h after PBS or flagellin administration as described in (A-C). (E) Quantitative analysis of CD86 expression in spleen *Tlr5*$^{-/-}$ and WT DC. (F) Representative plots of CD86 expression by *Tlr5*$^{-/-}$ and WT MdLN DC in response to intranasal injection of PBS or flagellin. (G) Mean CD86 expression in *Tlr5*$^{-/-}$ and WT MdLN DC. Data represent the mean ± SEM and are representative of 2-4 experiments (*$p<0.05$).

References

[1] Lycke N. Recent progress in mucosal vaccine development: potential and limitations. Nat Rev Immunol. 2012;12:592-605.

[2] Caskey M, Lefebvre F, Filali-Mouhim A, Cameron MJ, Goulet JP, Haddad EK, et al. Synthetic double-stranded RNA induces innate immune responses similar to a live viral vaccine in humans. J Exp Med. 2011;208:2357-66.

[3] Blander JM, Sander LE. Beyond pattern recognition: five immune checkpoints for scaling the microbial threat. Nat Rev Immunol. 2012;12:215-25.

[4] Buonaguro L, Pulendran B. Immunogenomics and systems biology of vaccines. Immunol Rev. 2011;239:197-208.

[5] Didierlaurent AM, Morel S, Lockman L, Giannini SL, Bisteau M, Carlsen H, et al. AS04, an aluminum salt- and TLR4 agonist-based adjuvant system, induces a transient localized innate immune response leading to enhanced adaptive immunity. J Immunol. 2009;183:6186-97.

[6] Mosca F, Tritto E, Muzzi A, Monaci E, Bagnoli F, Iavarone C, et al. Molecular and cellular signatures of human vaccine adjuvants. Proc Natl Acad Sci U S A. 2008;105:10501-6.

[7] Tritto E, Muzzi A, Pesce I, Monaci E, Nuti S, Galli G, et al. The acquired immune response to the mucosal adjuvant LTK63 imprints the mouse lung with a protective signature. J Immunol. 2007;179:5346-57.

[8] Kool M, Soullie T, van Nimwegen M, Willart MA, Muskens F, Jung S, et al. Alum adjuvant boosts adaptive immunity by inducing uric acid and activating inflammatory dendritic cells. J Exp Med. 2008;205:869-82.

[9] Didierlaurent AM, Collignon C, Bourguignon P, Wouters S, Fierens K, Fochesato M, et al. Enhancement of Adaptive Immunity by the Human Vaccine Adjuvant AS01 Depends on Activated Dendritic Cells. J Immunol. 2014;193:1920-30.

[10] Seubert A, Monaci E, Pizza M, O'Hagan DT, Wack A. The adjuvants aluminum hydroxide and MF59 induce monocyte and granulocyte chemoattractants and enhance monocyte differentiation toward dendritic cells. J Immunol. 2008;180:5402-12.

426 [11] Le Borgne M, Etchart N, Goubier A, Lira SA, Sirard JC, van Rooijen N, et al. Dendritic cells
427 rapidly recruited into epithelial tissues via CCR6/CCL20 are responsible for CD8+ T cell crosspriming
428 in vivo. Immunity. 2006;24:191-201.
429 [12] Randolph GJ, Jakubzick C, Qu C. Antigen presentation by monocytes and monocyte-derived
430 cells. Curr Opin Immunol. 2008;20:52-60.
431 [13] Meredith MM, Liu K, Darrasse-Jeze G, Kamphorst AO, Schreiber HA, Guermonprez P, et al.
432 Expression of the zinc finger transcription factor zDC (Zbtb46, Btbd4) defines the classical dendritic
433 cell lineage. J Exp Med. 2012;209:1153-65.
434 [14] Miller JC, Brown BD, Shay T, Gautier EL, Jojic V, Cohain A, et al. Deciphering the
435 transcriptional network of the dendritic cell lineage. Nat Immunol. 2012;13:888-99.
436 [15] Anandasabapathy N, Feder R, Mollah S, Tse SW, Longhi MP, Mehandru S, et al. Classical Flt3L-
437 dependent dendritic cells control immunity to protein vaccine. J Exp Med. 2014.
438 [16] Dalod M, Chelbi R, Malissen B, Lawrence T. Dendritic cell maturation: functional specialization
439 through signaling specificity and transcriptional programming. The EMBO journal. 2014;33:1104-16.
440 [17] Langlet C, Tamoutounour S, Henri S, Luche H, Ardouin L, Gregoire C, et al. CD64 expression
441 distinguishes monocyte-derived and conventional dendritic cells and reveals their distinct role during
442 intramuscular immunization. J Immunol. 2012;188:1751-60.
443 [18] Schlitzer A, McGovern N, Teo P, Zelante T, Atarashi K, Low D, et al. IRF4 transcription factor-
444 dependent CD11b+ dendritic cells in human and mouse control mucosal IL-17 cytokine responses.
445 Immunity. 2013;38:970-83.
446 [19] Furuhashi K, Suda T, Hasegawa H, Suzuki Y, Hashimoto D, Enomoto N, et al. Mouse lung
447 CD103+ and CD11bhigh dendritic cells preferentially induce distinct CD4+ T-cell responses. Am J
448 Respir Cell Mol Biol. 2012;46:165-72.
449 [20] Plantinga M, Guilliams M, Vanheerswynghels M, Deswarte K, Branco-Madeira F, Toussaint W,
450 et al. Conventional and monocyte-derived CD11b(+) dendritic cells initiate and maintain T helper 2
451 cell-mediated immunity to house dust mite allergen. Immunity. 2013;38:322-35.
452 [21] Pesce I, Monaci E, Muzzi A, Tritto E, Tavarini S, Nuti S, et al. Intranasal administration of CpG
453 induces a rapid and transient cytokine response followed by dendritic and natural killer cell activation
454 and recruitment in the mouse lung. J Innate Immun. 2010;2:144-59.

[22] Shi C, Pamer EG. Monocyte recruitment during infection and inflammation. Nat Rev Immunol. 2011;11:762-74.

[23] Schlitzer A, McGovern N, Teo P, Zelante T, Atarashi K, Low D, et al. IRF4 Transcription Factor-Dependent CD11b(+) Dendritic Cells in Human and Mouse Control Mucosal IL-17 Cytokine Responses. Immunity. 2013;38:970-83.

[24] Iijima N, Mattei LM, Iwasaki A. Recruited inflammatory monocytes stimulate antiviral Th1 immunity in infected tissue. Proc Natl Acad Sci U S A. 2011;108:284-9.

[25] Mizel SB, Bates JT. Flagellin as an adjuvant: cellular mechanisms and potential. J Immunol. 2010;185:5677-82.

[26] Didierlaurent A, Ferrero I, Otten LA, Dubois B, Reinhardt M, Carlsen H, et al. Flagellin promotes myeloid differentiation factor 88-dependent development of Th2-type response. J Immunol. 2004;172:6922-30.

[27] Kinnebrew MA, Buffie CG, Diehl GE, Zenewicz LA, Leiner I, Hohl TM, et al. Interleukin 23 production by intestinal CD103(+)CD11b(+) dendritic cells in response to bacterial flagellin enhances mucosal innate immune defense. Immunity. 2012;36:276-87.

[28] Uematsu S, Jang MH, Chevrier N, Guo Z, Kumagai Y, Yamamoto M, et al. Detection of pathogenic intestinal bacteria by Toll-like receptor 5 on intestinal CD11c+ lamina propria cells. Nat Immunol. 2006;7:868-74.

[29] Janot L, Sirard JC, Secher T, Noulin N, Fick L, Akira S, et al. Radioresistant cells expressing TLR5 control the respiratory epithelium's innate immune responses to flagellin. Eur J Immunol. 2009;39:1587-96.

[30] Van Maele L, Fougeron D, Janot L, Didierlaurent A, Cayet D, Tabareau J, et al. Airway structural cells regulate TLR5-mediated mucosal adjuvant activity. Mucosal Immunol. 2014;7:489-500.

[31] Wilson RH, Maruoka S, Whitehead GS, Foley JF, Flake GP, Sever ML, et al. The Toll-like receptor 5 ligand flagellin promotes asthma by priming allergic responses to indoor allergens. Nat Med. 2012;18:1705-10.

[32] Nempont C, Cayet D, Rumbo M, Bompard C, Villeret V, Sirard JC. Deletion of flagellin's hypervariable region abrogates antibody-mediated neutralization and systemic activation of TLR5-dependent immunity. J Immunol. 2008;181:2036-43.

[33] Barletta KE, Cagnina RE, Wallace KL, Ramos SI, Mehrad B, Linden J. Leukocyte compartments in the mouse lung: distinguishing between marginated, interstitial, and alveolar cells in response to injury. J Immunol Methods. 2012;375:100-10.

[34] Van Maele L, Carnoy C, Cayet D, Songhet P, Dumoutier L, Ferrero I, et al. TLR5 signaling stimulates the innate production of IL-17 and IL-22 by CD3(neg)CD127+ immune cells in spleen and mucosa. J Immunol. 2010;185:1177-85.

[35] Inaba K, Turley S, Iyoda T, Yamaide F, Shimoyama S, Reis e Sousa C, et al. The formation of immunogenic major histocompatibility complex class II-peptide ligands in lysosomal compartments of dendritic cells is regulated by inflammatory stimuli. J Exp Med. 2000;191:927-36.

[36] Honko AN, Mizel SB. Mucosal administration of flagellin induces innate immunity in the mouse lung. Infect Immun. 2004;72:6676-9.

[37] Munoz N, Van Maele L, Marques JM, Rial A, Sirard JC, Chabalgoity JA. Mucosal administration of flagellin protects mice from Streptococcus pneumoniae lung infection. Infect Immun. 2010;78:4226-33.

[38] Sporri R, Reis e Sousa C. Inflammatory mediators are insufficient for full dendritic cell activation and promote expansion of CD4+ T cell populations lacking helper function. Nat Immunol. 2005;6:163-70.

[39] Flores-Langarica A, Marshall JL, Hitchcock J, Cook C, Jobanputra J, Bobat S, et al. Systemic flagellin immunization stimulates mucosal CD103+ dendritic cells and drives Foxp3+ regulatory T cell and IgA responses in the mesenteric lymph node. J Immunol. 2012;189:5745-54.

[40] Hammad H, Chieppa M, Perros F, Willart MA, Germain RN, Lambrecht BN. House dust mite allergen induces asthma via Toll-like receptor 4 triggering of airway structural cells. Nat Med. 2009;15:410-6.

[41] Iwasaki A. Mucosal dendritic cells. Annu Rev Immunol. 2007;25:381-418.

[42] Lambrecht BN, Hammad H. Lung dendritic cells in respiratory viral infection and asthma: from protection to immunopathology. Annu Rev Immunol. 2012;30:243-70.

[43] Pang IK, Ichinohe T, Iwasaki A. IL-1R signaling in dendritic cells replaces pattern-recognition receptors in promoting CD8(+) T cell responses to influenza A virus. Nat Immunol. 2013;14:246-53.

[44] Tortola L, Rosenwald E, Abel B, Blumberg H, Schafer M, Coyle AJ, et al. Psoriasiform dermatitis is driven by IL-36-mediated DC-keratinocyte crosstalk. J Clin Invest. 2012;122:3965-76.

[45] Holt PG, Strickland DH, Wikstrom ME, Jahnsen FL. Regulation of immunological homeostasis in the respiratory tract. Nat Rev Immunol. 2008;8:142-52.

[46] Fahlen-Yrlid L, Gustafsson T, Westlund J, Holmberg A, Strombeck A, Blomquist M, et al. CD11c(high)dendritic cells are essential for activation of CD4+ T cells and generation of specific antibodies following mucosal immunization. J Immunol. 2009;183:5032-41.

[47] Calabro S, Tortoli M, Baudner BC, Pacitto A, Cortese M, O'Hagan DT, et al. Vaccine adjuvants alum and MF59 induce rapid recruitment of neutrophils and monocytes that participate in antigen transport to draining lymph nodes. Vaccine. 2011;29:1812-23.

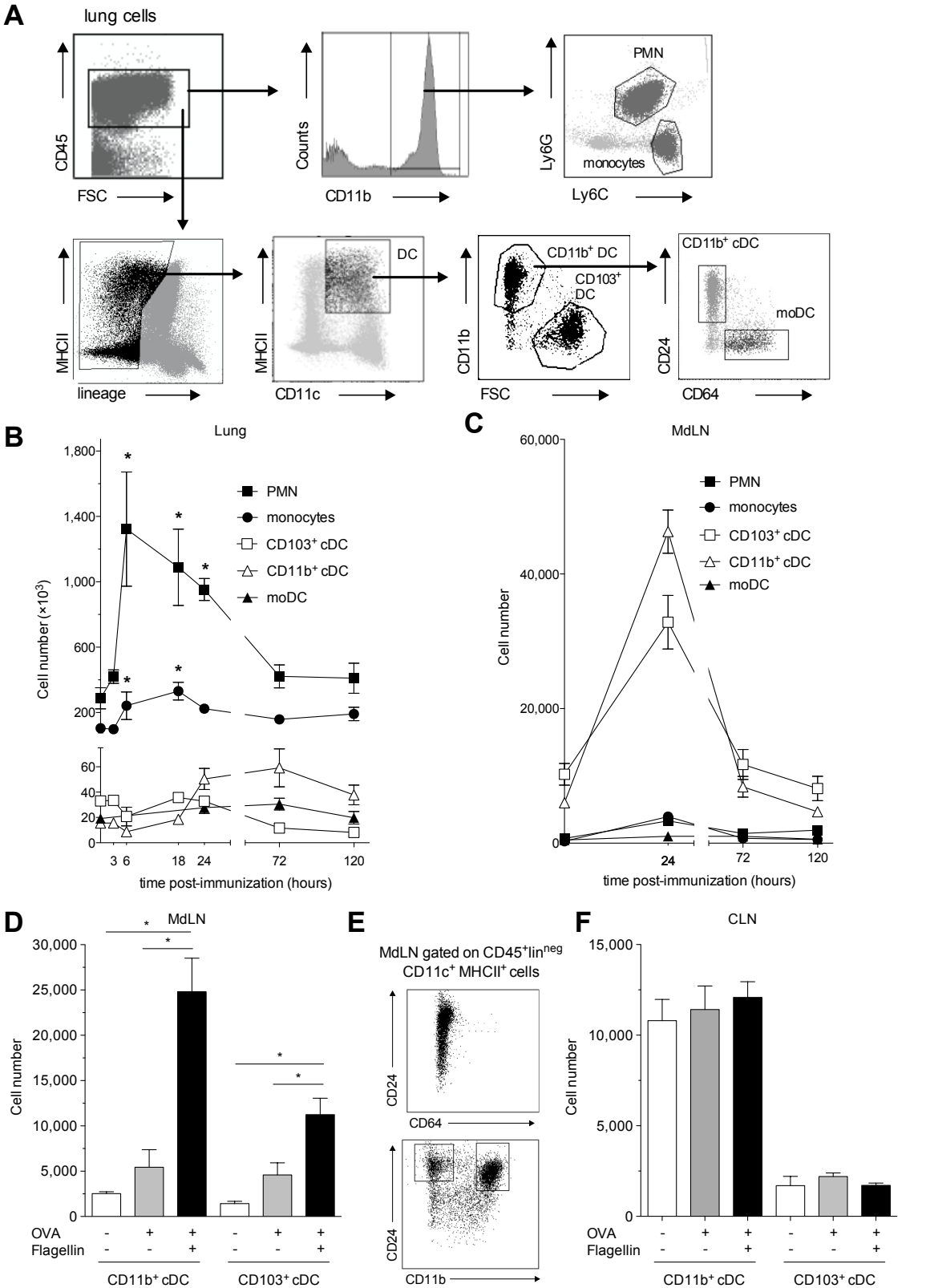

Figure 1: Fougeron *et al.*

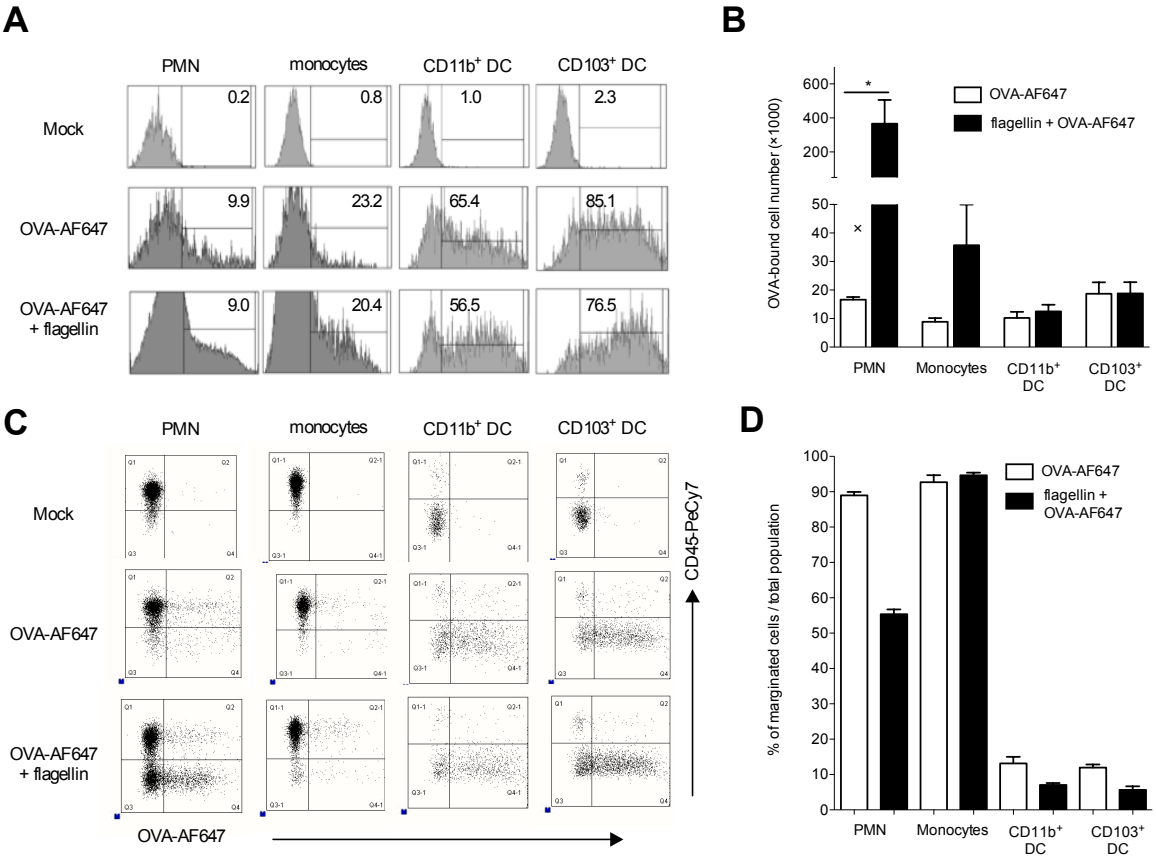

Figure 2: Fougeron *et al.*

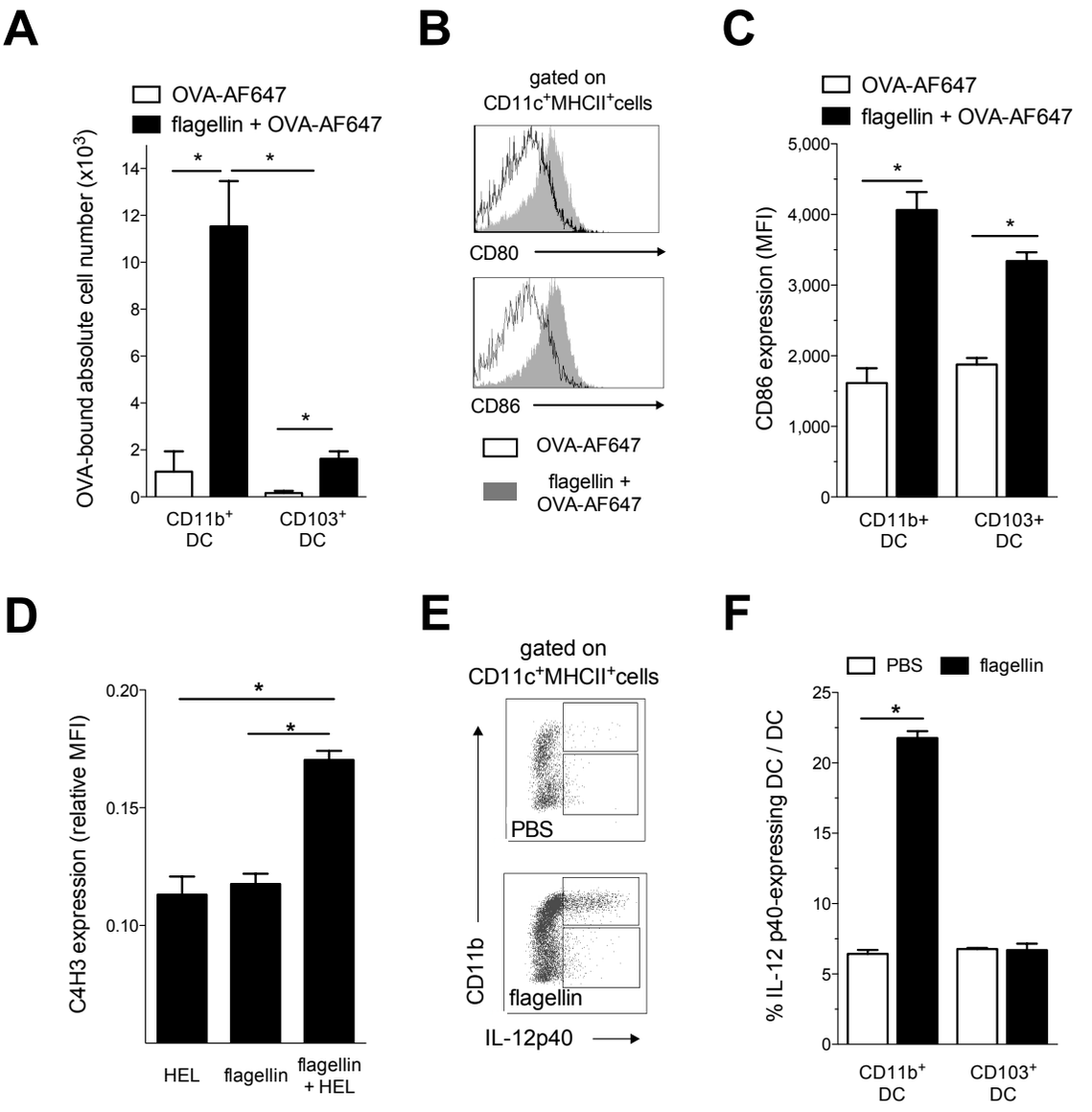

Figure 3: Fougeron *et al.*

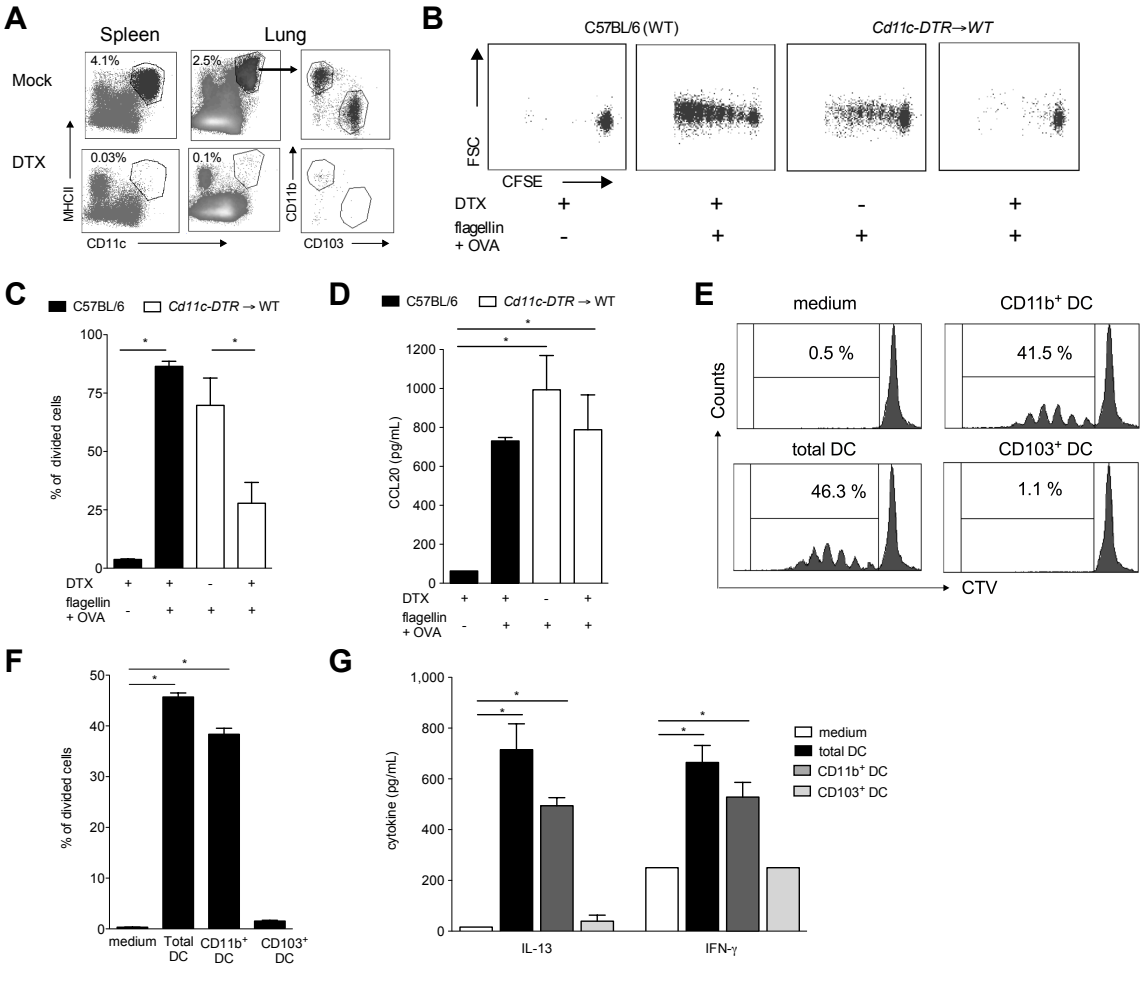

Figure 4: Fougeron *et al.*

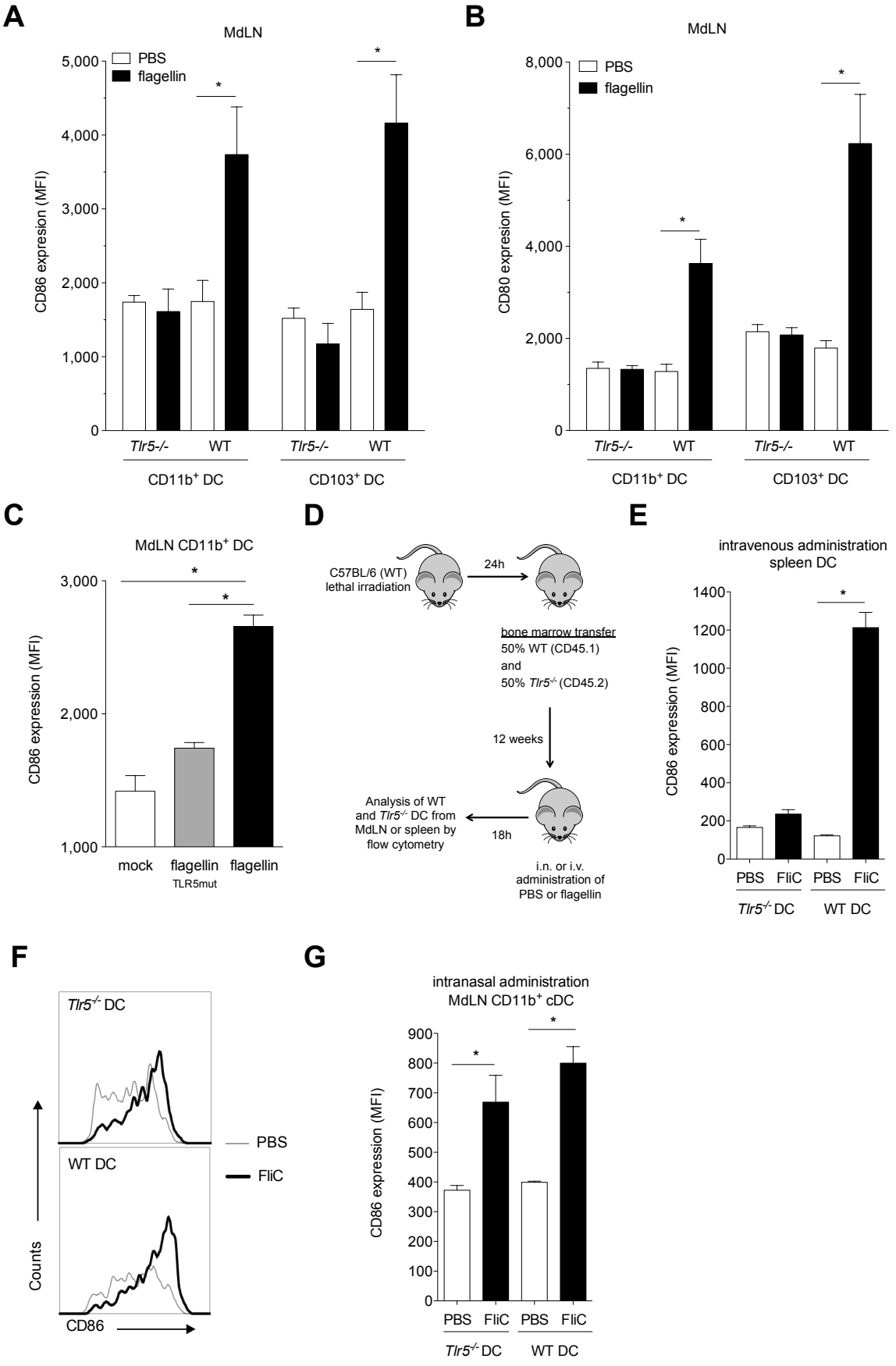

Figure 5 : Fougeron *et al.*

Conventional dendritic cells promotes the mucosal adjuvant activity of flagellin in the respiratory tract

Delphine Fougeron, Laurye Van Maele, Julien Tabareau, Pascal Songhet, Delphine Cayet, Nico Van Rooijen, David Hot, Hans-Joachim Mollenkopf, Wolf-Dietrich Hardt, Arndt G. Benecke, and Jean-Claude Sirard

This file includes Supplementary Materials and Methods, Supplementary Figures S1-S5, and Supplementary References

Supplementary Materials and Methods

Mice. Six to 10-weeks-old mice *Ccr2*$^{-/-}$, *Tlr5*$^{-/-}$ on the C57BL/6 background and NMRI mice were obtained from Taconic or bred in house. Broncho-alveolar lavages (BAL) were collected after the intra-tracheal injection of 1ml PBS with Protease Inhibitor Cocktail (Roche). Lung protein extracts were prepared by homogenizing tissue in Tissue Protein Extraction Reagent (Pierce) supplemented with protease inhibitors as described previouly [1, 2].

Neutrophil and monocyte depletions

Neutrophils were depleted by i.p. injection of anti-Ly6G (NIMP.R14, 200µg), or control isotype HB152 (rat IgG2b) as described previously [3]. Circulating monocytes were depleted by i.v. injection of clodronate liposome or empty liposomes [4]. Immunizations were performed 12h to 24h after the depletions.

Antigen-specific antibodies. Immunizations consisted in prime-boost at days 1 and 21 followed by serum sampling at day 28 for OVA-specific antibody titer determination. Levels of OVA-specific IgG were determined by ELISA as previously described [1]. Briefly, MaxiSorp microplates (Nunc) were coated overnight at 4°C with OVA (20µg per well in phosphate buffer 0.2M pH 6.5), washed with PBS/Tween20 0.05%, blocked with PBS/Dry Milk 1% for 1h, and washed again. Serial dilutions of samples were incubated for 1h, washed, and incubated for 1h with HRP-conjugated anti-mouse IgG (Southern Biotechnology Associates). After washing, development was done with 3,3',5,5' tetramethylbenzidine (Becton Dickinson Bioscience) and stopped by addition of H_2SO_4 and the OD at 450nm was determined. The IgG titer was defined as the reciprocal of the highest sample dilution yielding an absorbance value of 0.1 OD for OVA and was systematically compared with a reference serum.

Cell Culture. Mouse airway epithelial cells, both mouse tracheal epithelial cells and type II alveolar epithelial cells were differentiated from trachea and lungs of C57BL/6 mice, respectively, as described previously [5-7].

Gene expression. Total RNA from whole lung or cultured cells was extracted with Nucleospin RNA kits (Macherey-Nagel). RNA was reverse-transcribed with the High-Capacity cDNA Archive Kit (Applied Biosystems). cDNA was amplified using SYBR Green or TaqMan assays. Relative quantification was performed as described previously [8].

Antigen-specific cytokine production. OVA-specific T cell responses were analyzed in mice 7 days after the last immunization. Spleen cells ($2\text{-}5\times10^6$) were incubated for 72h with RPMI medium supplemented with 5% fecal calf serum ± OVA (1mg/mL) to measure secretion of IL-13 and IFN-γ.

Microarrays. Total lung RNA and blood RNA was extracted with the Nucleospin RNA kits (Macherey-Nagel). Lung RNA was processed on Applied Biosystems Mouse Whole Genome Arrays v2.0 and analyzed using the NeONORM method [9]. Blood RNA was processed on Agilent whole mouse genome microarrays and the Rosetta Resolver Biosoftware. Microarray data were MIAME compliant and deposited in the publicly available database:

http://mace.ihes.fr with accession number: 2176499768 and http://www.ncbi.nlm.nih.gov/geo/ with accession number: GSE46421. Gene lists containing group means of expression, p-values and standard fold changes were utilized as input for subsequent bioinformatics analysis. Genes belonging to the same biological functions/pathways were mapped using Ingenuity Pathway Analysis 1.0 (IPA, Ingenuity Systems), Kyoto Encyclopedia of Genes and Genomes (KEGG), and The Immunological Genome Project (www.immgen.org). Heat maps were generated using Gene-E (Broad Institute).

A

Type of cells	Model	% of depletion	
		Lung	Blood
PMN	NIMP.R14	100 %	100 %
Monocytes	Clodronate §	95±4%	97±2%

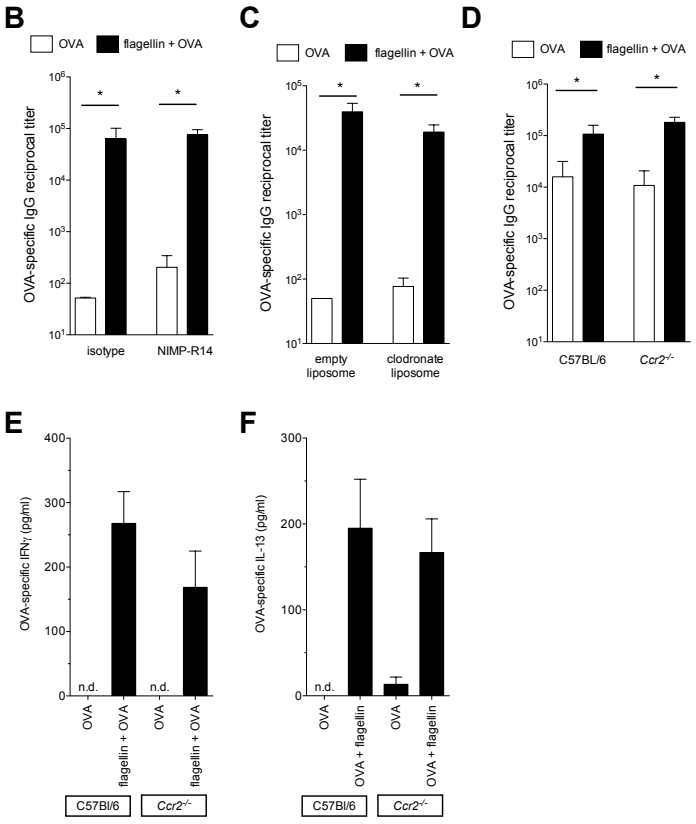

Figure S1. Monocytes and neutrophils are dispensable for flagellin-mediated adjuvant activity.

Neutrophils were depleted by i.p. injection of anti-Ly6G (NIMP.R14, 200µg), or control isotype HB152 (rat IgG2b, 200µg). Circulating monocytes were depleted by i.v. injection of clodronate liposome or empty liposomes. Immunizations were performed 12h to 24h after the depletions. (A) C57BL/6 and NMRI (§) mice were injected i.p. with Ly6G-specific depleting antibody NIMP.R14 or isotype HB152 (control), or i.v. with clodronate liposomes or empty liposomes (control). The percentage of depletion was measured with respects to control mice. Neutrophils ($CD45^+lin^{neg}CD11b^{high}Ly6C^+Ly6G^+$) and monocytes ($CD45^+lin^{neg}CD11b^{high}Ly6C^{high}Ly6G^{neg}$) were counted in the lung and in the blood after 12h to 24h. (B) NIMP.R14-depleted and isotype-treated C57BL/6 mice (n=7-8) were vaccinated i.n. at day 0 and day 21 either with ovalbumin (OVA) or flagellin plus OVA. OVA-specific IgG titer was determined in the serum at day 28. (C) NMRI mice (n=5-8) were injected i.v. with clodronate liposomes or empty liposomes and immunized i.n. with OVA or flagellin plus OVA. OVA-specific IgG titer was determined in the serum at day 21. (D-F) C57BL/6 and *Ccr2*$^{-/-}$ animals (n=8-9) (C) and (D) were vaccinated i.n. at day 0 and day 21 with OVA or flagellin plus OVA. OVA-specific IgG titers were measured by ELISA at day 28 (D). T cell secretion assays were performed on splenocytes stimulated with OVA for 3 days (E-F). Data are expressed as the mean ± SEM and are representative of 1-2 experiments. Statistical significance (*$p<0.05$) was determined using the Mann-Whitney test.

A

Lung canonical pathways	- log10(p value)		
	2h	4h	18h
Granulocyte Adhesion and Diapedesis	24.77	17.68	9.96
IL-10 Signaling	13.14	16.42	5.29
Acute Phase Response Signaling	13.21	14.69	5.6
Dendritic Cell Maturation	9.14	13.58	2.84
Activation of IRF by Cytosolic Pattern Recognition Receptors	5.86	13.74	0.87
TREM1 Signaling	11.80	10.38	2.82
IL-6 Signaling	10.09	9.89	2.65
NF-κB Signaling	12.18	9.21	2.58

B

Lung biological functions	- log10(p value)		
	2h	4h	18h
Function of leukocytes	54.67	60.87	15.09
Migration of blood cells	55.32	49.69	n.d.
Inflammatory response	53.46	49.34	18.75
Cell movement	46.32	34.44	15.79
Infiltration of cells	43.66	36.33	16,35
Function of antigen presenting cells	30.84	32.56	6.35
Adhesion of immune cells	32.89	33.12	14.12
Activation of antigen presenting cells	16.65	16.88	9.41

C

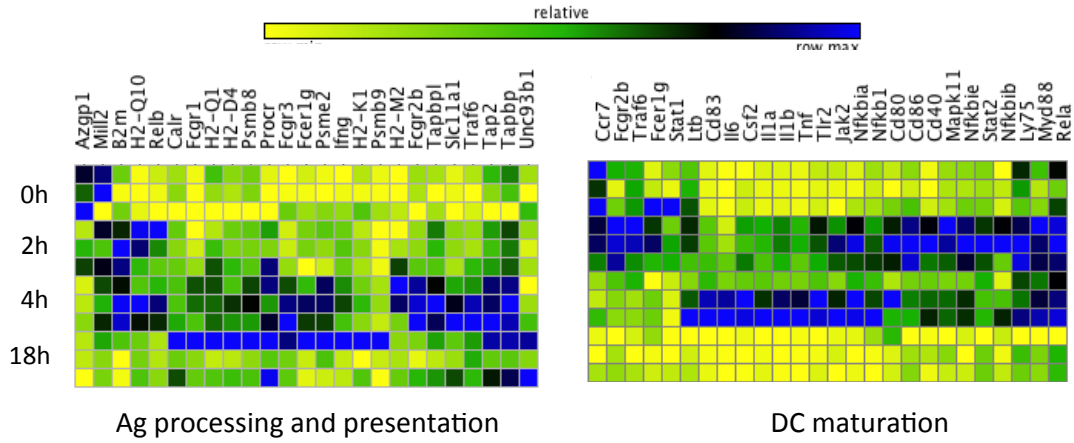

D

Blood canonical pathways	- log10(p value)		
	2h	4h	18h
IL-8 Signaling	1.25	5.54	0.55
Role of NFAT in Regulation of the Immune Response	n.d.	5.48	0.25
Superpathway of cholesterol Biosynthesis	0.70	0.63	5.43
JAK/Stat Signaling	0.35	4.64	0.27
CXCR4 Signaling	0.46	4.00	n.d.
IL-10 Signaling	n.d.	3.25	n.d.
Erythropoietin Signaling	0.37	3.19	n.d.
Fcγ Receptor-mediated Phagocytosis in Macrophages and Monocytes	0.77	2.92	n.d.

E

Blood biological functions	- log10(p value)		
	2h	4h	18h
Function of leukocytes	n.d.	13.76	n.d.
Migration of blood cells	n.d.	n.d.	n.d.
Inflammatory response	n.d.	8.48	n.d.
Cell movement	4.29	5.62	2.53
Infiltration of cells	n.d.	5.39	n.d.
Function of antigen presenting cells	n.d.	6.77	n.d.
Adhesion of immune cells	n.d.	5.04	n.d.
Activation of antigen presenting cells	n.d.	3.72	n.d.

Figure S2. The flagellin-specific lung but not blood response displays specific features of DC maturation. C57BL/6 mice (n=3-5 per group) were treated i.n. with flagellin for 2h, 4h, and 18h. Lung (A-C) and blood (D-E) whole-genome microarrays were analyzed. Differentially expressed genes with absolute fold change of expression > 2 relative to controls (0h) were used for analysis. (A-D, B-E) IPA analysis of microarray data. The significance is expressed as "-log(p-value)". (A, D) Main canonical pathways upregulated by flagellin in lung (A) and blood (D). (B, E) Main biological functions upregulated by flagellin in lung (B) and blood (E). (C) Heat maps of KEGG molecular functions and cell signatures established according to the Immgen database of lung tissue with respect to DC functions. Heat maps are based on average linkage method and Pearson Correlation as distance metric.

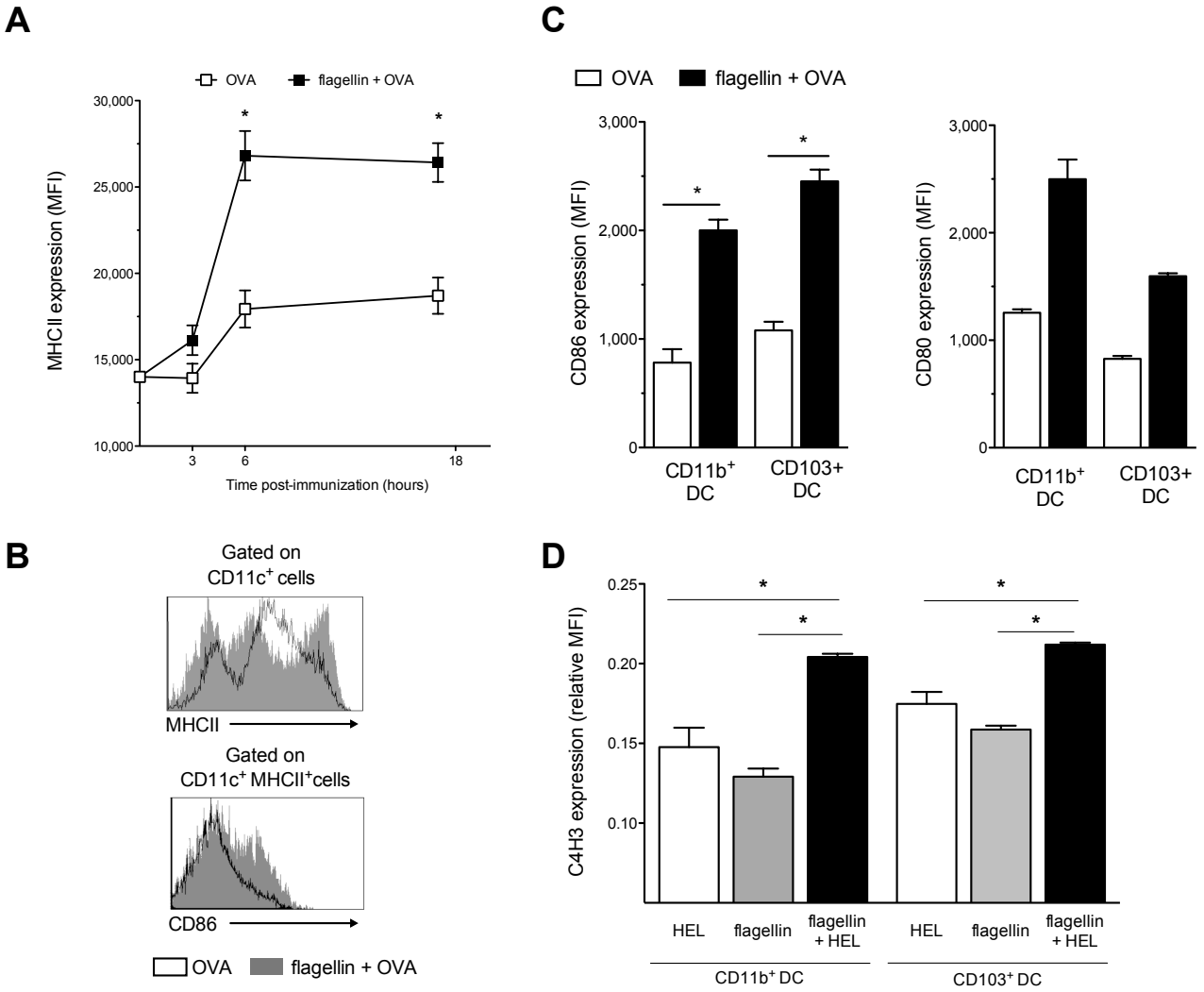

Figure S3. Intranasal administration of flagellin elicits the maturation of lung dendritic cells.

C57BL/6 (n=3-4) were immunized i.n. with ovalbumin OVA or flagellin and OVA. Lungs were sampled at indicated time for flow cytometry analysis. Dendritic cells were defined as $lin^{neg}CD45^{+}CD11c^{+}MHCII^{+}CD11b^{+/-}CD103^{+/-}$. (A) Expression of MHCII by lung total $CD11c^{+}$ cells over time. (B) Representative histograms of MHCII and CD86 expression by the indicated population in the lung. (C) Functional activation of lung $CD11b^{+}$ and $CD103^{+}$ DCs (CD86 and CD80 expression). Data are presented as the mean fluorescence intensity. (D) C3H/HeN animals (n=4) were immunized i.n. with either hen egg lysozyme (HEL), flagellin, or flagellin and HEL, and lungs were sampled 18h post administration. Antigen presentation by lung $CD11b^{+}$ and $CD103^{+}$ DCs was assessed with C4H3 antibody that detects HEL peptide loaded on $I\text{-}A^{k}$. Fluorescence of the C4H3 antibody was normalized against the $I\text{-}A^{k}$ fluorescence.

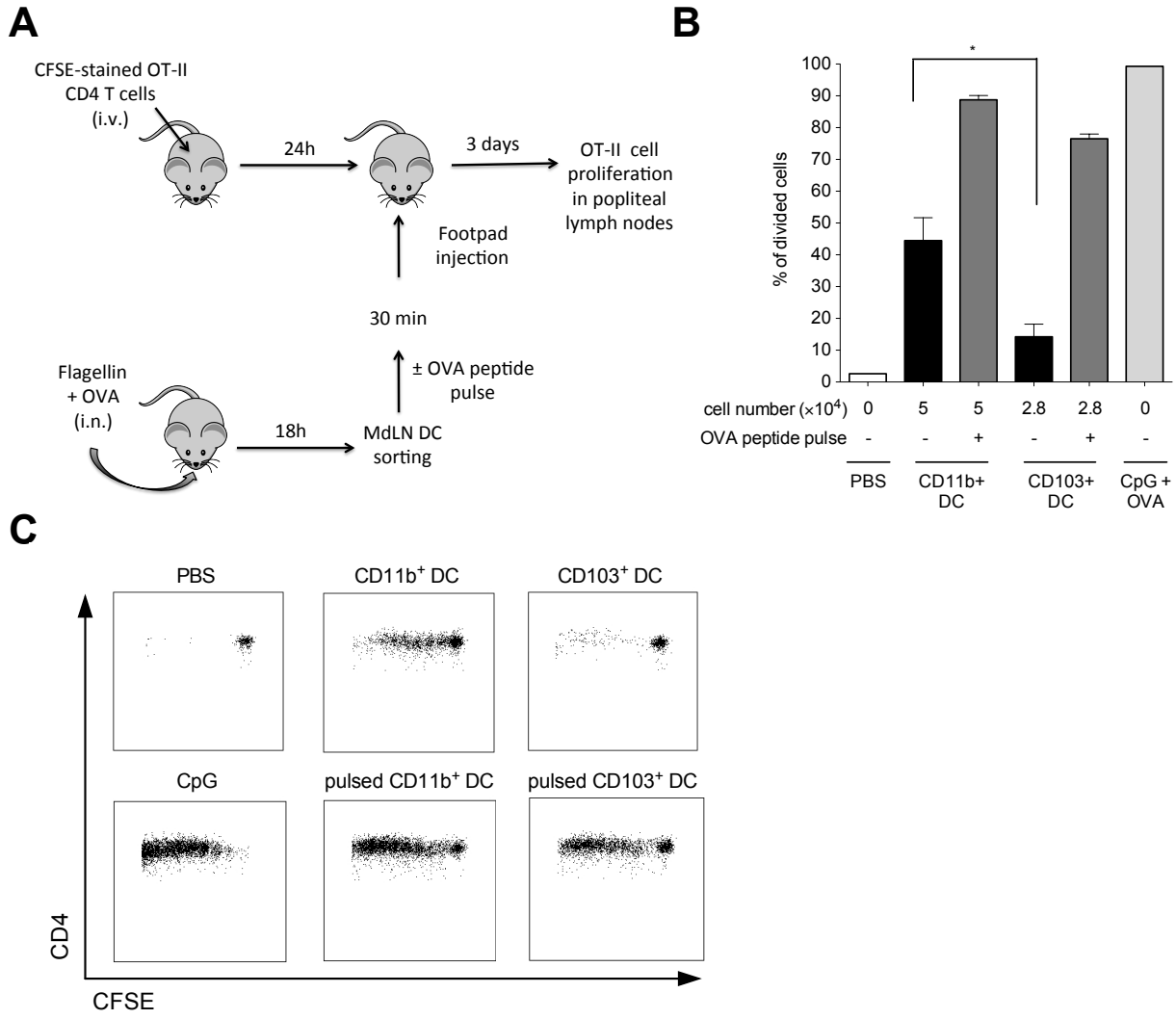

Figure S4. Mediastinal lymph node CD11b$^+$ dendritic cells from intranasally immunized animals present antigen to CD4 lymphocytes.

(A) Schematic representation of the protocol used for *ex vivo* antigen presentation assay. Naïve C57BL/6 mice (n=4 per group) were adoptively transferred with CFSE-labeled ovalbumin (OVA)-specific OT-II CD4$^+$ T cells 24h before immunization. (ii) C57BL/6 mice (n=16) were immunized i.n. with flagellin and OVA and the mediastinal lymph nodes (MdLN) were sampled 18h later. DCs (lin^{neg}CD45$^+$CD11c$^+$MHCII$^+$) were sorted as CD11b$^+$ and CD103$^+$ DC subsets and injected in the footpad of adoptively transferred recipient animals. With respects to their relative number in the MdLN, 5×10^4 CD11b$^+$ or 2.8×10^4 CD103$^+$ DC were respectively injected in recipient mice. In addition, 5×10^4 CD11b$^+$ or 2.8×10^4 CD103$^+$ DC loaded in vitro with OVA peptide (323-339) (denominated 'pulse') and CpG + OVA footpad immunization were used as positive controls. (B) Proliferation of CFSE-labeled OT-II T cells in the popliteal lymph nodes was analyzed 3 days after the injection (C) Representative dot plots of CFSE dilution of transferred OT-II cells induced by DCs or control treatment. Data are expressed as the mean ± SEM and are representative of 1-2 experiments. Statistical significance (*$p<0.05$) was determined using the Mann-Whitney test.

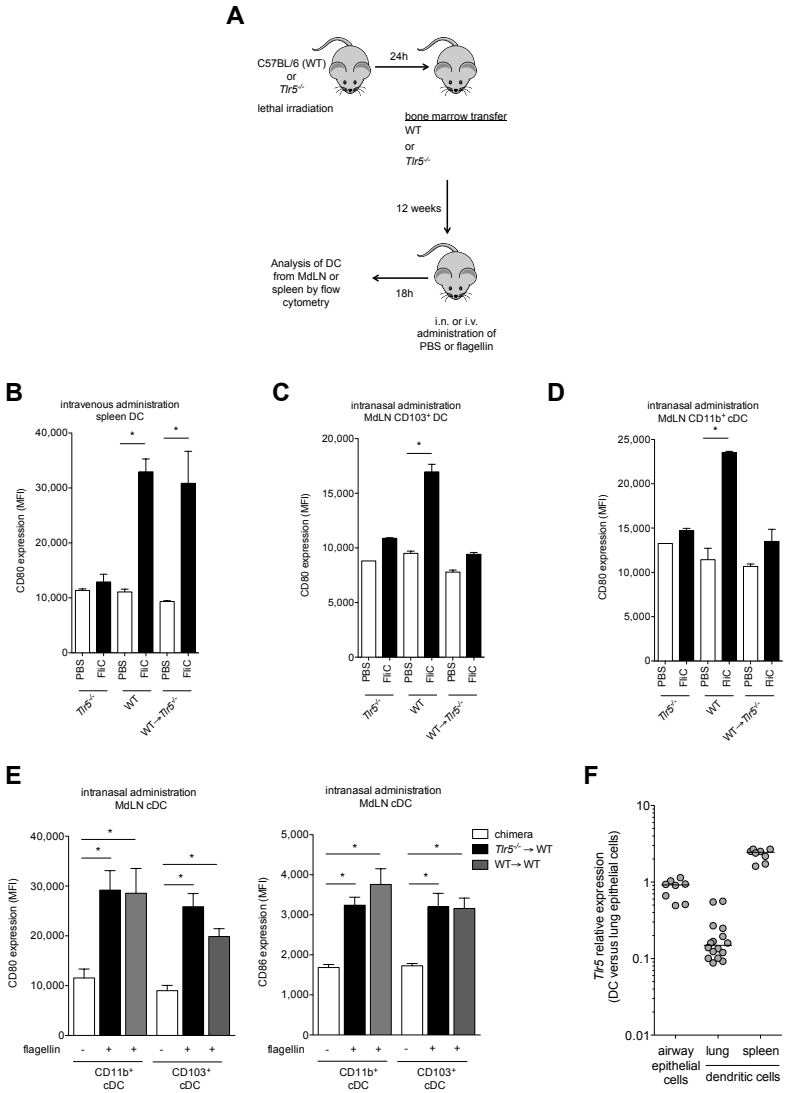

Figure S5. TLR5 expression in airway dendritic cell is not required for response to intranasal flagellin.

(A) Experimental strategy of bone marrow chimera. Bone marrow from *Tlr5*$^{-/-}$ or WT animals were injected into lethally irradiated *Tlr5*$^{-/-}$ or WT mice. Three months after engraftment (>95% reconstitution of DC compartment), chimera mice (n=3-5) were immunized with flagellin by intravenous (B) or intranasal (C-E) route. The maturation of spleen DC (B) or mediastinal lymph node (MdlN) DC (C-E) was assessed 18h after PBS or flagellin administration by flow cytometry analysis. Dendritic cells were defined as lin^{neg}CD45^{+}CD11c^{+}MHCII^{+}CD11b$^{+/-}$ CD103$^{+/-}$. (B) Quantitative analysis of CD80 expression by splenic DC in response to intravenous immunization. (C-E) Quantitative analysis of CD80 and CD86 expression by MdLN cDCs. (F) Total CD11c^{+}MHCII^{+} DC were sorted from lung or spleen of C57BL/6 mice. Airway epithelial cells were differentiated from mouse trachea and lung tissues. *Tlr5* mRNA levels were determined by quantitative PCR. Levels of mRNA in airway epithelial cells were arbitrarily set to 1 and used to calculate relative gene expression in spleen DC and lung DC. Data represent the mean ± SEM and are representative of 1-3 experiments (*p<0.05).

Supplementary references

[1] Nempont C, Cayet D, Rumbo M, Bompard C, Villeret V, Sirard JC. Deletion of flagellin's hypervariable region abrogates antibody-mediated neutralization and systemic activation of TLR5-dependent immunity. J Immunol. 2008;181:2036-43.
[2] Van Maele L, Fougeron D, Janot L, Didierlaurent A, Cayet D, Tabareau J, et al. Airway structural cells regulate TLR5-mediated mucosal adjuvant activity. Mucosal Immunol. 2014;7:489-500.
[3] Munoz N, Van Maele L, Marques JM, Rial A, Sirard JC, Chabalgoity JA. Mucosal administration of flagellin protects mice from Streptococcus pneumoniae lung infection. Infect Immun. 2010;78:4226-33.
[4] Van Rooijen N, Sanders A. Liposome mediated depletion of macrophages: mechanism of action, preparation of liposomes and applications. J Immunol Methods. 1994;174:83-93.
[5] Messier EM, Mason RJ, Kosmider B. Efficient and rapid isolation and purification of mouse alveolar type II epithelial cells. Experimental lung research. 2012;38:363-73.
[6] Crotta S, Davidson S, Mahlakoiv T, Desmet CJ, Buckwalter MR, Albert ML, et al. Type I and type III interferons drive redundant amplification loops to induce a transcriptional signature in influenza-infected airway epithelia. PLoS Pathog. 2013;9:e1003773.
[7] You Y, Richer EJ, Huang T, Brody SL. Growth and differentiation of mouse tracheal epithelial cells: selection of a proliferative population. American journal of physiology Lung cellular and molecular physiology. 2002;283:L1315-21.
[8] Van Maele L, Carnoy C, Cayet D, Songhet P, Dumoutier L, Ferrero I, et al. TLR5 signaling stimulates the innate production of IL-17 and IL-22 by CD3(neg)CD127+ immune cells in spleen and mucosa. J Immunol. 2010;185:1177-85.
[9] Noth S, Brysbaert G, Benecke A. Normalization using weighted negative second order exponential error functions (NeONORM) provides robustness against asymmetries in comparative transcriptome profiles and avoids false calls. Genomics Proteomics Bioinformatics. 2006;4:90-109.